Author Manuscript Published OnlineFirst on February 20, 2015; DOI: 10.1158/2326-6066.CIR-14-0190
Author manuscripts have been peer reviewed and accepted for publication but have not yet been edited.

MATERIALS AND METHODS

Mouse. Seven-week-old female C57BL/6 and male BALB/c mice were purchased from Japan SLC. Fluorescent ubiquitination-based cell cycle indicator (Fucci) double transgenic mice were generated by crossbreeding FucciG_1-#639 and FucciS/G_2/M-#474 animals (obtained from Dr. A. Miyawaki through the RIKEN BRC) as described previously (13). Mice transgenic for the gp100 melanoma antigen-specific Pmel-1-TCR or the ovalbumin specific OT-I TCR were purchased from The Jackson Laboratory. Each experimental group contained 8 mice except where otherwise specified. All animal experiments were conducted in accordance with institutional guidelines with the approval of the Animal Care and Use Committee of the University of Tokyo.

Cell lines and tumor models. B16F10 and LLC were obtained from the American Type Culture Collection. Colon 26 was obtained from the Cell Resource Center for Biomedical Research, Institute of Development, Aging, and Cancer, Tohoku University. B16F10 cells expressing the truncated form of human low-affinity nerve growth factor receptor (ΔhLNGFR/hCD271) were generated by retroviral transduction and 2 subsequent rounds of *in vivo* passaging (Supplementary Fig. S1). B16F10 cells (5×10^5 per mouse), LLC cells (5×10^5 per mouse) and Colon 26 cells (2×10^5 per mouse) were inoculated s.c. into the right flanks of C57BL/6 or BALB/c mice. Tumor diameter was measured twice weekly and used to calculate tumor volume (mm^3) [(major axis; mm) × (minor axis; mm) ^{2} × 0.5236].

***In vivo* antibody treatment.** Anti-CD4 (clone GK1.5), anti-CD8 (clone YTS169.4), anti-PD-1 (clone J43), anti-PD-L1 (clone 10F.9G2), anti-PD-L2 (clone TY25), anti-OX40 (clone OX-86), anti-CTLA-4 (clone 9D9), anti-LAG-3 (clone C9B7W), anti-BTLA (clone 6A6), anti-TIM-3 (clone RMT3-23), anti-GITR (clone DTA-1) and anti-CD25 (clone PC-61.5.3) mAbs were purchased from BioXcell. Antibodies were injected intraperitoneally at a dose of 200 μg per mouse. Anti-CD4 mAb (200 μg/mouse) was administered in a single dose or in successive doses on days 5 and 9 after tumor inoculation. Immune checkpoint antibodies (200 μg/mouse) were administered on days 4, 8, 14 and 18 after tumor-inoculation. Combination treatments with the anti-CD4 mAb and anti-immune checkpoint antibodies were administered under the same conditions as respective single agent protocols.

Immunohistological analysis. Immunofluorescent staining was performed as described previously (14-16) using primary antibodies and the appropriate fluorophore-conjugated secondary Abs as listed in Table S1, then photographed using a SP5 confocal microscope (Leica Microsystems).

Flow cytometry. Intravascular leukocytes were stained by intravenous injection of fluorophore-conjugated mAb (3 μg/mouse) against CD45 or CD45.2 3 min prior to collecting tissues. Single-cell suspensions were prepared by enzymatic or mechanical dissociation of tissues with or without subsequent density separation, as described previously (17, 18). Flow-Count fluorospheres (Beckman Coulter) were used to determine cell numbers and normalize cell concentrations prior to antibody staining. Cells were pretreated with Fc Block (anti-mouse CD16/CD32 mAb; clone 2.4G2, BioXcell), then stained with mix of fluorophore-conjugated anti-mouse mAbs as indicated in Table S1. Data were acquired on a Gallios flow cytometer (Beckman Coulter) and analyzed using FlowJo software (version 9.7.5; FlowJo, LLC). Non-viable cells were excluded from the analysis based on forward and side scatter profiles and propidium iodide staining.

Quantitative reverse transcription real-time polymerase chain reaction. Total RNA was extracted using a RNeasy Mini kit (Qiagen) and converted to cDNA using ReverTra Ace qPCR RT Master Mix with gDNA Remover (Toyobo) according to the manufacturer's instructions. Real-time quantitative PCR analysis was performed using THUNDERBIRD Probe qPCR Mix or THUNDERBIRD SYBR qPCR Mix (Toyobo) and an ABI 7500 sequence detector system (Life Technologies). The primers used for the PCR reaction are listed in Table S2. The expression levels of each gene were normalized to *Rps3* expression level for each sample.

Statistics. Unless otherwise stated, data are presented as mean ± SE. Statistical analyses were performed using GraphPad Prism software (version 6.0e, GraphPad Software). For comparisons between groups in the *in vivo* study we used one-way ANOVA with Dunnett's post-hoc test. For comparisons between the means of two variables we used paired Student's *t*-tests. Comparisons of survival data between groups were made using the log-rank test after Kaplan-Meier analysis. A P-value < 0.05 was considered to be statistically significant.

Author Manuscript Published OnlineFirst on February 20, 2015; DOI: 10.1158/2326-6066.CIR-14-0190
Author manuscripts have been peer reviewed and accepted for publication but have not yet been edited.

RESULTS

An optimized anti-CD4 mAb treatment protocol exerts robust antitumor effects

We began by optimizing the protocol for anti-CD4 mAb administration in B16F10, Lewis lung carcinoma (LLC) and Colon 26 tumor models. Mice bearing subcutaneous tumors received a single intraperitoneal injection of 200 μg anti-CD4 mAb 2 days before (day –2) or 0, 3, 5 or 9 days after tumor inoculation. In all three models, administration of anti-CD4 mAb on days 3 and 5 significantly suppressed tumor growth (Supplementary Fig. S2A–C). B16F10 tumor growth, but not LLC and Colon 26 tumor growth, was also inhibited by mAb administration on days –2 and 0 (Supplementary Fig. S2A). However, the growth of LLC and Colon 26 tumors was not significantly affected by mAb administration at days –2 and 0 (Supplementary Fig. S2B and C). Successive administration of the anti-CD4 mAb on days 5 and 9 resulted in the greatest inhibition of tumor growth in all three models (data not shown). Doses of anti-CD4 mAb (3.1 or 12.5 μg/mouse) that were insufficient to cause CD4 lymphocyte depletion had no inhibitory effect on tumor growth in the melanoma model (Supplementary Fig. S2D and E). Based on these results, for subsequent studies we adopted a protocol of administering the anti-CD4 mAb at a dose of 200 μg/mouse successively on days 5 and 9 after tumor inoculation.

We next compared the antitumor effects of the anti-CD4 mAb against those of a variety of immune checkpoint mAbs (PD-1, PD-L1, PD-L2, CTLA-4, OX40, LAG-3, TIM-3, BTLA and GITR) in the B16F10 model, because melanoma is a major target of anti-immune checkpoint antibody therapy. We found that twice-weekly injections of immune checkpoint antibodies were sufficient to produce the same level of anti-tumor effect as achieved with daily injections (data not shown). Among the mAbs tested, the anti-CD4 mAb was the most effective single-agent treatment in terms of tumor growth inhibition and survival (Fig. 1A–C). Collectively, these results confirm the potent antitumor effects of anti-CD4 mAb treatment in mice and reveal a surprising advantage of anti-CD4 mAb treatment over immune checkpoint mAb treatment.

Anti-CD4 mAb treatment depletes $CD4^+$ T cells and pDCs

To determine which cells are depleted by anti-CD4 mAb therapy, we next examined changes in cell populations with immunosuppressive potential following anti-CD4 mAb administration at day 5 in mice bearing B16F10 tumors. Flow cytometric analysis revealed that numbers of $CD4^+$ T cells including $Foxp3^+CD25^+$ Tregs decreased 50- to 100-fold over days 2 to 9 following anti-CD4 mAb administration (7 to 14 days after tumor inoculation), as compared to cell numbers in phase-matched untreated tumor-bearing mice (Supplementary Fig. S3A–C). When LLC tumor-bearing mice were administered anti-CD4 mAb on days 5 and 9,

Author Manuscript Published OnlineFirst on February 20, 2015; DOI: 10.1158/2326-6066.CIR-14-0190
Author manuscripts have been peer reviewed and accepted for publication but have not yet been edited.

199 $CD4^+$ T cells disappeared from the blood until at least day 15 after the first mAb administration
200 (Supplementary Fig. S3D). pDCs, a subset of which are positive for CD4 and have been
201 implicated in the suppression of antitumor immune responses (7), also decreased 3- to 10-fold
202 over days 2 to 9 following mAb treatment (Supplementary Fig. S3A–C). MDSC subpopulations,
203 including neutrophils and Ly-$6C^{hi}$ or Ly-$6C^{lo}$ monocytes, were not significantly affected by mAb
204 treatment (data not shown). These results indicate that $CD4^+$ T cells (including Tregs) and pDCs
205 are the targets of anti-CD4 mAb therapy.
206
207 **Anti-CD4 mAb treatment increases the number of tumor-infiltrating $CD8^+$ T cells**
208 We next investigated the effects of anti-CD4 mAb therapy on tumor-infiltrating $CD8^+$
209 T-cell populations. Intravascular staining (IVS) is a technique that allows circulating leukocytes
210 present in tissue blood vessels (which represent a proportion of total leukocytes recovered) to be
211 distinguished from cells actually infiltrating the parenchyma of tissues, including tumors (19).
212 In untreated B16F10 tumors, about 15% of $CD8^+$ T cells were positive for IVS, and the
213 frequency of PD-$1^+$$CD137^+$ tumor-reactive cells (20) was about 10-fold lower in this population
214 than in the IVS-negative parenchymal cell population (Supplementary Fig. S4A and B).
215 Anti-CD4 mAb treatment significantly increased the frequency and number of IVS-$CD45^-$ $CD8^+$
216 T cells in the tumor (Fig. 2A and B). The increased number of $CD8^+$ T cells in the tumors of
217 anti-CD4 mAb-treated mice was also evident in histological sections (Fig. 2C). Furthermore, the
218 IVS^-CD8^+ T cells induced by anti-CD4 mAb treatment contained a higher proportion of
219 PD-$1^+$$CD137^+$ tumor-reactive cells (Fig. 2D and E), had greater potential to produce IFNγ in
220 response to *ex vivo* PMA/ionomycin stimulation (Fig. 2F and G), and showed higher specific
221 killing activity against B16F10 tumor cells (Supplementary Fig. S5A–C), compared to T cells
222 from the untreated group. In the LLC and Colon 26 tumor models, anti-CD4 mAb-treated mice
223 displayed decreased tumor growth, systemically increased $CD8^+CD44^{hi}$PD-1^+ T cells, and
224 upregulation of LAG-3, TIM-3, and CTLA-4 in tumor-infiltrating $CD8^+$ T cells (Supplementary
225 Fig. S6A–D). Collectively, these results suggest that anti-CD4 mAb treatment enhances
226 antitumor $CD8^+$ T-cell responses and induces a shift towards type I immunity within the tumor.
227
228 **Anti-CD4 mAb treatment promotes expansion of tumor-specific $CD8^+$ T cells in the**
229 **draining lymph node**
230 To further investigate the effects of anti-CD4 mAb treatment on tumor-specific $CD8^+$
231 T-cell responses, we adoptively transferred melanoma antigen-specific Pmel-1 TCR transgenic
232 $CD8^+$ T cells (21) into mice 1 day before inoculation with B16F10 tumors (day –1)
233 (Supplementary Fig. S7A and B). On day 14 after tumor inoculation, numbers of Pmel-1 $CD8^+$
234 T cells in the blood, draining lymph node (dLN), non-dLN (ndLN), spleen and tumor were 10-

Author Manuscript Published OnlineFirst on February 20, 2015; DOI: 10.1158/2326-6066.CIR-14-0190
Author manuscripts have been peer reviewed and accepted for publication but have not yet been edited.

to 100-fold higher in anti-CD4 mAb-treated mice compared to that in untreated mice (Supplementary Fig. S7C and D). As tumors grew, Pmel-1 $CD8^+$ T-cell numbers were unchanged or decreased in untreated group mice, whereas Pmel-1 $CD8^+$ T-cell numbers increased in anti-CD4 mAb-treated mice (Supplementary Fig. S7E). To determine the site of Pmel-1 $CD8^+$ T-cell expansion, we administered BrdU one hour prior to collecting tissues. The number of $BrdU^+$ proliferating Pmel-1 $CD8^+$ T cells in the dLN far outnumbered those in the tumor, irrespective of anti-CD4 mAb treatment (Supplementary Fig. S7F and G). Importantly, proliferating cell numbers decreased between days 9 and 14 in untreated mice, but increased in anti-CD4 mAb-treated mice (Supplementary Fig. S7H). Similar CD4-depletion-induced proliferation was also observed in endogenous polyclonal $CD8^+$ T cells (data not shown). These data suggest that anti-CD4 mAb treatment protects tumor-reactive $CD8^+$ T cells from deletion, a mechanism of peripheral tolerance in which the continuous and excessive exposure of antigen-specific T cells to cognate antigens eventually results in the loss of the antigen-specific T-cell clones.

To confirm the effects of anti-CD4 mAb treatment on the proliferation of $CD8^+$ T cells, we used fluorescent ubiquitination-based cell-cycle indicator (Fucci) double transgenic mice. In Fucci mice, Fucci-orange (mKO2) and Fucci-green (mAG) are expressed reciprocally in the G_0/G_1 and $S/G_2/M$ phases of the cell cycle, respectively (13, 18). In the B16F10 tumor model, anti-CD4 mAb treatment significantly increased the proportion of mAG^+ proliferating cells among $CD8^+CD44^{hi}$ T cells in both the dLN and non-dLN, compared to the proportion of these cells in untreated control mice (Supplementary Fig. S7I and J).

To determine whether this CD4 depletion-induced proliferation was specific for tumor-specific $CD8^+$ T cells or was a tumor antigen-independent response such as homeostatic proliferation (22), we adoptively transferred a CFSE-labeled mixture of Pmel-1, ovalbumin-specific OT-I and polyclonal $CD8^+$ T cells into B16 tumor-bearing or tumor-free mice with or without anti-CD4 mAb treatment (Supplementary Fig. S8A). Pmel-1 but not OT-I or polyclonal $CD8^+$ T cells selectively proliferated in the dLN of B16 tumor-bearing mice (Supplementary Fig. S8B–E). These results indicate that CD4 depletion-induced T-cell expansion is specific for tumor-specific $CD8^+$ T cells. Collectively, these results suggest that anti-CD4 mAb treatment systemically increases the availability of tumor-specific $CD8^+$ T cells by enhancing their proliferation in the dLN in a tumor-associated antigen-dependent manner.

Enhanced $CD8^+$ T-cell responses underlie the antitumor effects of anti-CD4 mAb treatment

To determine whether enhanced CTL responses are responsible for the antitumor effects of anti-CD4 mAb treatment, we administered the anti-CD4 mAb together with an

Author Manuscript Published OnlineFirst on February 20, 2015; DOI: 10.1158/2326-6066.CIR-14-0190
Author manuscripts have been peer reviewed and accepted for publication but have not yet been edited.

anti-CD8-depleting mAb. When the anti-CD8-depleting mAb was administered together with the anti-CD4 mAb, the inhibitory effect of anti-CD4 mAb treatment on tumor growth was completely reversed (Fig. 3A and B). We also investigated whether treatment with an anti-CD25-depleting mAb, which is widely used to deplete $Foxp3^+CD25^+$ Tregs in mice (23), could produce the same effect as anti-CD4 mAb treatment. Under our administration protocol, tumor growth in the anti-CD25 mAb-treated group was almost equivalent to that observed in untreated mice (Fig. 3A and B). These results suggest that the tumor-specific $CD8^+$ T cells that are induced by CD4 mAb treatment are responsible for the antitumor effects of the treatment, and that anti-CD4 mAb treatment might deplete immunosuppressive populations more efficiently than anti-CD25 mAb treatment.

Combination treatment with anti-CD4 and anti-PD-1 or anti-PD-L1 mAbs synergistically enhances antitumor effects

Next, we examined whether synergistic antitumor effects could be achieved by supplementing anti-CD4 mAb treatment with various immune checkpoint mAbs, particularly those targeting the exhaustion and deletion phase of the immune response. We devised a combination treatment protocol of anti-CD4 mAb with immune checkpoint antibodies as depicted in Fig. 4A. Strikingly, combination treatment with anti-CD4 and anti-PD-L1 mAbs, and to a lesser extent anti-CD4 and anti-PD-1 mAbs, resulted in dramatic synergistic inhibition of tumor growth in the B16F10 melanoma model (Fig. 4B and C). Combination treatment with anti-CD4 and anti-CTLA-4, anti-TIM-3, anti-BTLA and anti-GITR mAbs also had additive or synergistic effects (Fig. 4B and C), but anti-PD-L2, anti-OX40 and anti-LAG-3 mAbs produced no synergistic antitumor effect when combined with the anti-CD4 mAb (Fig. 4B and C). Survival was also prolonged by combination treatment with anti-CD4 and anti-PD-L1 mAbs compared to anti-CD4 mAb monotherapy, but not by other combinations of anti-CD4 and immune checkpoint mAbs (Fig. 4D). Importantly, depletion of $CD8^+$ T cells completely abrogated the tumor growth inhibition induced by the combination of anti-CD4 and anti-PD-1 or PD-L1 mAbs, indicating that $CD8^+$ T cells play a critical role in the antitumor effects of the combination treatment (Fig. 4E).

To determine whether the synergistic antitumor effects of anti-CD4 and anti-PD-1 or anti-PD-L1 mAb treatment are common to other tumor types and mouse strains, we examined the effect of combination treatment in the Colon 26 subcutaneous tumor model in BALB/c mice. The anti-PD-1 or anti-PD-L1 mAb treatment alone did not inhibit tumor growth, whereas combination treatment with anti-CD4 and anti-PD-1 or anti-PD-L1 mAbs resulted in strong synergistic inhibition of tumor growth (Fig. 5A and B). These effects were completely reversed by treatment with an anti-CD8 depleting mAb (Fig. 5B). Notably, we observed complete

Author Manuscript Published OnlineFirst on February 20, 2015; DOI: 10.1158/2326-6066.CIR-14-0190
Author manuscripts have been peer reviewed and accepted for publication but have not yet been edited.

remission in three of ten mice treated with the anti-CD4/anti-PD-1 mAb combination, and in six of ten mice treated with the anti-CD4/anti-PD-L1 mAb combination. In addition, the six mice that rejected the tumor in the anti-CD4/anti-PD-L1 mAb-treated group were resistant to re-challenge with Colon 26 tumor cells at a dose 5 times higher than that used in the initial inoculation (Fig. 5C). Collectively, these results indicate that combination treatment with anti-CD4 and anti-PD-1 or anti-PD-L1 mAbs has a dramatic and robust antitumor effect that is mediated by antitumor $CD8^+$ T cells.

Blockade of the PD-1/PD-L1 signaling axis increases the number of PD-1^+ tumor-reactive $CD8^+$ T cells in the circulation

Finally, we investigated the cellular and molecular mechanisms underlying the synergy between anti-CD4 and anti-PD-1 or anti-PD-L1 mAbs in the B16F10 melanoma model. Quantitative RT-PCR analysis of whole tumor tissue demonstrated that anti-CD4 mAb treatment alone augmented expression of the antitumor cytokine genes *Ifng* and *Tnf*, the IFNγ-inducible genes *Cxcl10* and *Cd274*/PD-L1 (24, 25), and genes encoding the pro-apoptotic molecules *Fasl*, *Prf1*/perforin, and *Gzmb*/Granzyme B, compared with the expression levels of these genes in untreated tumors (Supplementary Fig. S9A and B). The upregulation of PD-L1 by anti-CD4 mAb treatment was also observed at the protein level (Supplementary Fig. S9C). However, no additive or synergistic effects on gene expression were observed in groups receiving combination treatment with anti-CD4 and anti-PD-1 or PD-L1 mAbs. Consistent with these results, the proportion of IFNγ-producing and TNFα-producing cells within the tumor-infiltrating $CD8^+$ T-cell population was equivalent between mice receiving anti-CD4 mAb alone and mice receiving the combination of anti-CD4 and anti-PD-1 or anti-PD-L1 mAbs (data not shown).

We next analyzed the effects of anti-PD-1 and anti-PD-L1 mAbs on the PD-1^+CD8^+ T cells that increase in number in the systemic circulation in response to anti-CD4 mAb treatment. We examined cell populations expressing the effector/memory T-cell marker CD44 and the activation marker CD137. Combination treatment with anti-CD4 and anti-PD-L1 mAbs increased the frequency of $CD44^{hi}$PD-1^+ cells amongst $CD8^+$ T cells in the blood, dLN and non-dLN, compared to that in mice receiving the anti-CD4 mAb alone (blood data shown in Fig. 6A and B). In blood $CD8^+$ T cells, expression levels of PD-1 on cells within the $CD44^{hi}$PD-1^+ population and the frequency of PD-1^+CD137^+ cells were significantly higher in mice that received the combination of anti-CD4 and anti-PD-L1 mAbs compared to the corresponding expression levels and frequency in mice that received the anti-CD4 mAb alone (Fig. 6A–C). In contrast, combination treatment with anti-CD4 and anti-PD-1 mAbs decreased the frequency of the $CD44^{hi}$PD-1^+ population among blood $CD8^+$ T cells, and decreased the expression levels of

Author Manuscript Published OnlineFirst on February 20, 2015; DOI: 10.1158/2326-6066.CIR-14-0190
Author manuscripts have been peer reviewed and accepted for publication but have not yet been edited.

PD-1 on cells within the $CD44^{hi}$ $PD\text{-}1^{+}$ population (Fig. 6A, E and F). However, the frequency of the $CD44^{hi}CD137^{+}$ tumor-reactive cell population was higher in mice receiving the combination of anti-CD4 and anti-PD-1 mAbs compared to mice receiving the anti-CD4 mAb alone (Fig. 6A, E and F), suggesting that anti-PD-1 mAb treatment does not actually decrease the number of tumor-reactive $CD8^{+}$ T cells in the blood, but rather decreases the level of PD-1 expression on these cells. On the other hand, the frequency of $PD\text{-}1^{+}$ cells among tumor-infiltrating $CD8^{+}$ T cells in anti-CD4 mAb-treated mice was not affected by treatment with anti-PD-1 or anti-PD-L1 mAbs (Fig. 6D and G).

Author Manuscript Published OnlineFirst on February 20, 2015; DOI: 10.1158/2326-6066.CIR-14-0190
Author manuscripts have been peer reviewed and accepted for publication but have not yet been edited.

DISCUSSION

The recent success of anti-CTLA-4 and anti-PD-1 mAb therapies in the clinic has highlighted the potential of immunotherapy for the treatment of cancer (2, 3, 26-29). However, the development of immunotherapy for widespread clinical use remains in its early stages. Extensive efforts have been directed toward enhancing endogenous antitumor immunity by dampening the influence of immunosuppressive mechanisms. Treatment strategies have included combinations of antibodies with other antibodies and with other immunotherapies or anti-cancer therapeutics. In the present study, we demonstrate that antibody-mediated depletion of $CD4^+$ cells from tumor-bearing mice results in enhanced polyclonal PD-1^+CD137^+ tumor-reactive and monoclonal tumor-specific Pmel-1 $CD8^+$ T-cell responses, and strong inhibition of tumor growth. Combination treatment with the anti-CD4 mAb and various immune checkpoint mAbs, particularly anti-PD-1 and anti-PD-L1 mAbs, revealed striking synergy in suppressing tumor growth and prolonging survival.

Several previous reports have described antitumor activity of anti-CD4 mAb treatment in solid tumor models in C57BL/6 mice, including subcutaneous tumors induced by inoculation with B16 melanoma cells (9, 11, 12), recurrent TC1 lung cancer cells (30), or embryo cells expressing the adenovirus-derived E1A protein (10). Although the efficacy of immunotherapy in mouse tumor models often depends on tumor type, taken together, these reports from independent groups and our results from the present study suggest that anti-CD4 mAb treatment is likely to have broad spectrum antitumor activity against solid tumors. Optimization of the anti-CD4 mAb administration protocol revealed robust antitumor effects when mice received the mAb on days 3 or 5, rather than when mice receive the mAb prior to tumor inoculation (day –2). These results suggest that pretreatment is not necessary. However, priming and/or the pre-existence of activated $CD8^+$ T cells are important for effective anti-CD4 mAb therapy. Although the mechanistic link between the timing of anti-CD4 antibody administration and the efficacy of treatment remains to be elucidated, administration of the antibody to patients with early-stage cancer or whose tumor burden has been reduced by surgical resection, irradiation or chemotherapeutics is likely to be most beneficial.

A dose of anti-CD4 mAb sufficient to deplete most $CD4^+$ cells was required in order for antitumor effects to be observed. The $CD4^+$ cell population includes $Foxp3^+$ $CD25^+$ Tregs, Th2 cells, Tr1/3 cells (4) and IDO^+ immunosuppressive pDCs (7). Considering that markedly increased proliferation of tumor-specific $CD8^+$ T cells was observed in the dLN, anti-CD4 mAb treatment is likely to augment proliferation of tumor-reactive $CD8^+$ T cells through the removal of these $CD4^+$ immunosuppressive cells from the dLN. In addition, anti-CD4 mAb treatment increased the proportion of PD-1^+CD137^+ tumor-reactive cells and IFNγ-producing cells among tumor-infiltrating $CD8^+$ T cells in the B16F10 model, suggesting that anti-CD4 mAb treatment

Author Manuscript Published OnlineFirst on February 20, 2015; DOI: 10.1158/2326-6066.CIR-14-0190
Author manuscripts have been peer reviewed and accepted for publication but have not yet been edited.

augmented both the quantity and quality of tumor-specific $CD8^+$ T-cell responses. We recently demonstrated that IFNγ- and TNFα-induced cell-cycle arrest is an important mechanism underlying the antitumor effects induced by tumor-specific $CD8^+$ T-cell transfer (31). The shift towards IFNγ-dominant type I immunity, which was evident in the strong induction of IFNγ and TNFα in tumor-infiltrating $CD8^+$ T cells after anti-CD4 mAb treatment, is likely to play a central role in the antitumor effects that we observed (32). Notably, depletion of $CD25^+$ Tregs by administration of an anti-CD25 mAb on days 5 and 9 post tumor inoculation did not reproduce the antitumor effect of anti-CD4 mAb treatment. Because some $Foxp3^+$ Tregs have low-to-negative CD25 expression, residual $Foxp3^+ CD25^{-/lo}$ Tregs may have contributed to this discrepancy. Moreover, the antitumor effects of anti-CD25 mAb treatment have been reported to be optimal when the mAb is administered prior to tumor inoculation (33, 34), because when administered after tumor inoculation the anti-CD25 mAb depletes not only Tregs but also other activated lymphocytes expressing CD25. The involvement of Treg and other $CD4^+$ immunosuppressive populations in the suppression of $CD8^+$ T cell-mediated antitumor responses remains to be elucidated.

The synergy that occurs in combination treatment with anti-CD4 and anti-PD-1 or anti-PD-L1 mAbs is likely due to the blockade of PD-1/PD-L1 signaling in $PD\text{-}1^+$ activated $CD8^+$ T cells that are induced by anti-CD4 mAb treatment. We did not detect any synergistic effect in terms of the quantity and quality of the tumor-infiltrating $CD8^+$ T-cell response promoted by anti-CD4 and anti-PD-1 or anti-PD-L1 mAb treatment. However, the frequency of the $PD\text{-}1^+CD137^+$ and $CD44^{hi}CD137^+$ tumor-reactive populations increased among $CD8^+$ T cells in the blood upon blockade of the PD-1/PD-L1 signaling axis. Considering that T cells continuously traffic between peripheral and secondary lymphoid tissues via the lymph-blood circulation, the blockade of PD-1/PD-L1 signaling may prevent exhaustion or deletion of tumor-reactive $PD\text{-}1^+CD8^+$ T cells in the tumor and allow them to migrate into the dLN, thus sustaining antitumor $CD8^+$ T-cell responses. In addition, anti-CD4 mAb treatment increased the number of IFNγ-producing $PD\text{-}1^+$ $CD8^+$ T cells in the tumor, resulting in the upregulation of IFNγ-inducible genes including PD-L1. Although the shift towards IFNγ-dominant type-1 immunity within the tumor contributes to the inhibition of tumor growth, it also promotes the exhaustion or deletion of tumor-infiltrating $PD\text{-}1^+CD8^+$ T cells by enhancing PD-1/PD-L1 signaling. It is therefore likely that the synergy of the anti-CD4 and anti-PD-1 or anti-PD-L1 mAb combination treatment arises due to the blockade of this adverse negative feedback mechanism.

We are in the process of developing a humanized anti-CD4 mAb with potent antibody-dependent cell-mediated cytotoxicity (ADCC) as an anti-cancer therapeutic. Because $CD4^+$ T cells play important roles in both humoral and cellular immunity, the heightened risk of

Author Manuscript Published OnlineFirst on February 20, 2015; DOI: 10.1158/2326-6066.CIR-14-0190
Author manuscripts have been peer reviewed and accepted for publication but have not yet been edited.

infectious diseases that may be associated with transient $CD4^+$ T-cell depletion should be carefully evaluated in clinical trials. In addition, trials should seek to maximize clinical efficacy and safety through rigorous optimization of the antibody administration protocol. In pre-clinical studies in nonhuman primates, no serious adverse effects were detected after several weeks of treatment with our humanized anti-human CD4 mAb that resulted in $CD4^+$ T-cell depletion. In addition, no severe adverse effects have been observed during phase-II clinical trials for T-cell malignancy with long-term administration of other humanized anti-CD4 mAbs (35, 36). Preexisting humoral immune mediators, such as immunoglobulin, plasma cells and memory B cells, $CD8^+$ T-cell responses, and unimpaired natural immunity are likely to provide basal protection against infectious diseases during $CD4^+$ T cell-depleting therapies. On the other hand, consideration should also be given to the potential for the acute exacerbation of chronic diseases associated with viral infection (e.g. hepatitis C and B) due to excessive activation of effector and memory $CD8^+$ T cells after $CD4^+$ cell depletion.

In conclusion, our study represents the first report of robust antitumor effects of combination treatment with an anti-CD4-depleting antibody and anti-PD-1 or anti-PD-L1 immune checkpoint antibodies in mice. We have also characterized the immunologic bases for the synergy between these agents. Recent clinical trials suggest that anti-PD-1, anti-PD-L1, or anti-CTLA-4 mAbs, or combinations of these agents, are not effective against all types of solid tumors. Our findings suggest that combination treatment with an anti-CD4 mAb and immune checkpoint mAbs, particularly anti-PD-1 or anti-PD-L1 mAbs, is likely to result in greater clinical efficacy against a broader ranges of cancers.

444 **ACKNOWLEDGMENTS**

445 We thank A. Miyawaki, A. Sakaue-Sawano and the RIKEN BioResource Center for providing
446 FucciG1 and FucciS/G2/M mice; A. Hosoi for assistance with Pmel-1-B16F10 experiments; H.
447 Yamazaki, K. Tsuji, and K. Yoshioka for animal care; A. Yamashita, S. Aoki and S. Fujita for
448 expert technical assistance; and M. Otsuji, K. Takeda and S. Shibayama for helpful discussions.

449

450 **FOOTNOTES**

451 Author contributions: S.Y., S.U., Y.I., S.I. and K.M. designed research; S.Y., S.U., Y.I., H.O.,
452 K.C., T.N., K.H., Y.T., E.T., A.H. performed research; S.Y., S.U., Y.I., H.O., K.C., S.S., K.K., S.I.
453 and K.M. analyzed data; S.Y., S.U., Y.I., K.C., F.H.W.S., K.K., S.I. and K.M. wrote the paper.

Author Manuscript Published OnlineFirst on February 20, 2015; DOI: 10.1158/2326-6066.CIR-14-0190
Author manuscripts have been peer reviewed and accepted for publication but have not yet been edited.

REFERENCES

1. Pardoll DM. The blockade of immune checkpoints in cancer immunotherapy. Nat Rev Cancer. 2012;12:252-64.
2. Topalian SL, Weiner GJ, Pardoll DM. Cancer immunotherapy comes of age. J Clin Oncol. 2011;29:4828-36.
3. Wolchok JD, Kluger H, Callahan MK, Postow MA, Rizvi NA, Lesokhin AM, et al. Nivolumab plus ipilimumab in advanced melanoma. N Engl J Med. 2013;369:122-33.
4. Whiteside TL. Disarming suppressor cells to improve immunotherapy. Cancer Immunol Immunother. 2012;61:283-8.
5. Alizadeh D, Larmonier N. Chemotherapeutic targeting of cancer-induced immunosuppressive cells. Cancer Res. 2014;74:2663-8.
6. Camisaschi C, De Filippo A, Beretta V, Vergani B, Villa A, Vergani E, et al. Alternative activation of human plasmacytoid DCs in vitro and in melanoma lesions: involvement of LAG-3. J Invest Dermatol. 2014;134:1893-902.
7. Matta BM, Castellaneta A, Thomson AW. Tolerogenic plasmacytoid DC. European J Immunol. 2010;40:2667-76.
8. Nagai H, Hara I, Horikawa T, Fujii M, Kurimoto M, Kamidono S, et al. Antitumor effects on mouse melanoma elicited by local secretion of interleukin-12 and their enhancement by treatment with interleukin-18. Cancer Invest. 2000;18:206-13.
9. Nagai H, Hara I, Horikawa T, Oka M, Kamidono S, Ichihashi M. Elimination of CD4(+) T cells enhances anti-tumor effect of locally secreted interleukin-12 on B16 mouse melanoma and induces vitiligo-like coat color alteration. J Invest Dermatol. 2000;115:1059-64.
10. den Boer AT, van Mierlo GJ, Fransen MF, Melief CJ, Offringa R, Toes RE. CD4+ T cells are able to promote tumor growth through inhibition of tumor-specific CD8+ T-cell responses in tumor-bearing hosts. Cancer Res. 2005;65:6984-9.
11. Yu P, Lee Y, Liu W, Krausz T, Chong A, Schreiber H, et al. Intratumor depletion of CD4+ cells unmasks tumor immunogenicity leading to the rejection of late-stage tumors. The Journal of experimental medicine. 2005;201:779-91.
12. Choi BK, Kim YH, Kang WJ, Lee SK, Kim KH, Shin SM, et al. Mechanisms involved in synergistic anticancer immunity of anti-4-1BB and anti-CD4 therapy. Cancer Res. 2007;67:8891-9.
13. Sakaue-Sawano A, Kurokawa H, Morimura T, Hanyu A, Hama H, Osawa H, et al. Visualizing spatiotemporal dynamics of multicellular cell-cycle progression. Cell. 2008;132:487-98.
14. Ueha S, Yoneyama H, Hontsu S, Kurachi M, Kitabatake M, Abe J, et al. CCR7

490 mediates the migration of Foxp3+ regulatory T cells to the paracortical areas of peripheral
491 lymph nodes through high endothelial venules. J Leukoc Biol. 2007;82:1230-8.
492 15. Ueha S, Murai M, Yoneyama H, Kitabatake M, Imai T, Shimaoka T, et al.
493 Intervention of MAdCAM-1 or fractalkine alleviates graft-versus-host reaction associated
494 intestinal injury while preserving graft-versus-tumor effects. J Leukoc Biol. 2007;81:176-85.
495 16. Shono Y, Ueha S, Wang Y, Abe J, Kurachi M, Matsuno Y, et al. Bone marrow
496 graft-versus-host disease: early destruction of hematopoietic niche after MHC-mismatched
497 hematopoietic stem cell transplantation. Blood. 2010;115:5401-11.
498 17. Sawanobori Y, Ueha S, Kurachi M, Shimaoka T, Talmadge JE, Abe J, et al.
499 Chemokine-mediated rapid turnover of myeloid-derived suppressor cells in tumor-bearing
500 mice. Blood. 2008;111:5457-66.
501 18. Shand FH, Ueha S, Otsuji M, Koid SS, Shichino S, Tsukui T, et al. Tracking of
502 intertissue migration reveals the origins of tumor-infiltrating monocytes. ProcNatl Acad Sci
503 U S A. 2014;111:7771-6.
504 19. Anderson KG, Mayer-Barber K, Sung H, Beura L, James BR, Taylor JJ, et al.
505 Intravascular staining for discrimination of vascular and tissue leukocytes. Nat Protoc.
506 2014;9:209-22.
507 20. Ye Q, Song DG, Poussin M, Yamamoto T, Best A, Li C, et al. CD137 accurately
508 identifies and enriches for naturally occurring tumor-reactive T cells in tumor. Clin Cancer
509 Res. 2014;20:44-55.
510 21. Overwijk WW, Theoret MR, Finkelstein SE, Surman DR, de Jong LA, Vyth-Dreese
511 FA, et al. Tumor regression and autoimmunity after reversal of a functionally tolerant state
512 of self-reactive CD8+ T cells. J Exp Med. 2003;198:569-80.
513 22. Surh CD, Sprent J. Homeostasis of naive and memory T cells. Immunity.
514 2008;29:848-62.
515 23. Sakaguchi S. Regulatory T cells: history and perspective. Methods Mol Biol.
516 2011;707:3-17.
517 24. Dong H, Strome SE, Salomao DR, Tamura H, Hirano F, Flies DB, et al.
518 Tumor-associated B7-H1 promotes T-cell apoptosis: a potential mechanism of immune
519 evasion. Nature Med. 2002;8:793-800.
520 25. Furuta J, Inozume T, Harada K, Shimada S. CD271 on melanoma cell is an
521 IFN-gamma-inducible immunosuppressive factor that mediates downregulation of
522 melanoma antigens. J Invest Dermatol. 2014;134:1369-77.
523 26. Couzin-Frankel J. Breakthrough of the year 2013. Cancer immunotherapy. Science.
524 2013;342:1432-3.
525 27. Hamid O, Robert C, Daud A, Hodi FS, Hwu WJ, Kefford R, et al. Safety and tumor

526 responses with lambrolizumab (anti-PD-1) in melanoma. The New England journal of
527 medicine. 2013;369:134-44.
528 28. Topalian SL, Drake CG, Pardoll DM. Targeting the PD-1/B7-H1(PD-L1) pathway to
529 activate anti-tumor immunity. Curr Opin Immunol. 2012;24:207-12.
530 29. Topalian SL, Hodi FS, Brahmer JR, Gettinger SN, Smith DC, McDermott DF, et al.
531 Safety, activity, and immune correlates of anti-PD-1 antibody in cancer. N Engl J Med.
532 2012;366:2443-54.
533 30. Predina J, Eruslanov E, Judy B, Kapoor V, Cheng G, Wang LC, et al. Changes in
534 the local tumor microenvironment in recurrent cancers may explain the failure of vaccines
535 after surgery. Proc Natl Acad Sci U S A. 2013;110:E415-24.
536 31. Matsushita H, Hosoi A, Ueha S, Abe J, Fujieda N, Tomura M, et al. Cytotoxic T
537 lymphocytes block tumor growth both by lytic activity and IFN-gamma-dependent cell cycle
538 arrest. Cancer Immunol Res. 2015;3:26-36.
539 32. Braumuller H, Wieder T, Brenner E, Assmann S, Hahn M, Alkhaled M, et al.
540 T-helper-1-cell cytokines drive cancer into senescence. Nature. 2013;494:361-5.
541 33. Onizuka S, Tawara I, Shimizu J, Sakaguchi S, Fujita T, Nakayama E. Tumor
542 rejection by in vivo administration of anti-CD25 (interleukin-2 receptor alpha) monoclonal
543 antibody. Cancer Res. 1999;59:3128-33.
544 34. Shimizu J, Yamazaki S, Sakaguchi S. Induction of tumor immunity by removing
545 CD25+CD4+ T cells: a common basis between tumor immunity and autoimmunity. J
546 Immunol. 1999;163:5211-8.
547 35. Kim YH, Duvic M, Obitz E, Gniadecki R, Iversen L, Osterborg A, et al. Clinical
548 efficacy of zanolimumab (HuMax-CD4): two phase 2 studies in refractory cutaneous T-cell
549 lymphoma. Blood. 2007;109:4655-62.
550 36. Rider DA, Havenith CE, de Ridder R, Schuurman J, Favre C, Cooper JC, et al. A
551 human CD4 monoclonal antibody for the treatment of T-cell lymphoma combines inhibition
552 of T-cell signaling by a dual mechanism with potent Fc-dependent effector activity. Cancer
553 Res. 2007;67:9945-53.
554
555

Author Manuscript Published OnlineFirst on February 20, 2015; DOI: 10.1158/2326-6066.CIR-14-0190
Author manuscripts have been peer reviewed and accepted for publication but have not yet been edited.

FIGURE LEGENDS

Figure 1. Antitumor effects of anti-CD4 mAb treatment.

Mice bearing B16F10 melanoma tumors were injected intraperitoneally with anti-CD4 mAb (200 μg/mouse) on days 5 and 9 or anti-immune checkpoint mAbs on days 4, 8, 14 and 18 after tumor inoculation. (A) Tumor growth curves. (B) Tumor volume on day 16 (upper panel) or day 15 (lower panel). (C) Survival following tumor inoculation (8 mice per group). (A, B) Data represent mean ± SE of 8 mice per group. *, $P < 0.05$; **, $P < 0.01$; ***, $P < 0.001$ (compared to control).

Figure 2. Anti-CD4 mAb treatment increases the number of tumor-infiltrating $CD8^+$ T cells.

Mice bearing B16F10 (A, B, D–G) or B16F10-ΔhLNGFR (C) tumors were injected intraperitoneally with anti-CD4 mAb on days 5 and 9, and tumor-infiltrating $CD8^+$ T cells were analyzed on day 14 after tumor inoculation. Control mice received an injection of vehicle only. For flow cytometric analyses, mice were given an intravenous injection of anti-CD45.2 Ab 3 min prior to the collection of tissues to enable identification of cells in the blood compartment (intravascular staining, IVS). (A) Flow cytometry plots of parenchymal leukocyte compartments ($CD45^+$ IVS-$CD45.2^-$). (B) The number of parenchymal $CD8^+$ T cells in tumor. (C) Distribution of $CD8^+$ T cells in the tumor. Green, CD8; red, ΔhLNGFR; blue, propidium iodide (PI). Enlargements in white boxes show non-necrotic areas, yellow box shows necrotic area. Scale bar represents 200 μm. (D) Flow cytometry plots and (E) frequencies of PD-1^+ $CD137^+$ tumor-reactive cells among the parenchymal $CD8^+$ T-cell population. (F) Flow cytometry plots and (G) frequencies of IFNγ- and TNFα-producing cells among the parenchymal $CD8^+$ T-cell population following *ex vivo* re-stimulation with PMA and ionomycin. Data represent mean ± SE of 4 mice per group and are representative of at least four independent experiments. Numbers in flow cytometry plots indicate mean frequencies within live cells (A) or parental populations (D and F). ***, $P < 0.001$ (compared to control).

Figure 3. $CD8^+$ T cells play a pivotal role in the antitumor effects of anti-CD4 mAb treatment.

Mice bearing B16F10 tumors were injected intraperitoneally with anti-CD4, anti-CD8 and/or anti-CD25 mAbs (200 μg/mouse) on days 5 and 9 after tumor inoculation. (A) Tumor growth curves. (B) Tumor volume on day 15 after tumor inoculation. Data represent mean ± SE of 8 mice per group. **, $P < 0.05$ (compared to control); ††, $P < 0.01$ (comparison as indicated).

Figure 4. Combination treatment with anti-CD4 and anti-PD-1 or anti-PD-L1 mAbs has

Author Manuscript Published OnlineFirst on February 20, 2015; DOI: 10.1158/2326-6066.CIR-14-0190
Author manuscripts have been peer reviewed and accepted for publication but have not yet been edited.

synergistic antitumor effects.

Mice bearing B16F10 tumors received anti-CD4 mAb, anti-immune checkpoint mAb, or a combination of these, according to the treatment schedule shown in (A). (B) Tumor volume on day 16 (left) or 15 (right). *, $P < 0.05$; **, $P < 0.01$; ***, $P < 0.001$ (compared to control); #, $P=0.021$ (compared to αCD4); ††, $P < 0.01$; †††, $P < 0.001$ (comparisons as indicated). (C) Tumor growth curves. (D) Survival plots representative of two independent experiments. *, $P < 0.05$; **, $P < 0.01$ ***, $P < 0.001$ ****, $P < 0.0001$ (compared to control); †, $P < 0.05$; ††, $P < 0.01$; †††, $P < 0.001$ (compared to αCD4). (E) Anti-CD8 mAb was administered together with anti-CD4 mAb and tumor volumes were measured on day 16. **, $P < 0.01$ (compared to control). Data represent mean ± SE of 8 mice per group. In the text as (data not shown) but should insert into Figure 4.

Figure 5. Combination treatment with anti-CD4 and anti-PD-1 or anti-PD-L1 mAbs induces long-term antitumor $CD8^+$ T-cell memory.

Mice bearing Colon 26 tumors received anti-CD4, anti-PD-L1, anti-PD-1 or anti-CD8 mAbs or a combination of these according to the treatment schedule shown in Fig. 4A. (A) Tumor growth curves. (B) Tumor volume on day 18. **, $P < 0.01$; ***, $P < 0.001$ (compared to control); #, $P=0.029$; ###, $P < 0.001$ (compared to αCD4); †††, $P < 0.001$ (comparisons as indicated). (C) The six mice that achieved complete remission of Colon 26 tumors after anti-CD4 and anti-PD-L1 treatment were re-challenged on day 39 with Colon 26 tumor cells at five-times the cell number of the initial challenge. Arrow indicates day of re-challenge. *, $P < 0.05$; **, $P < 0.01$ (compared to control). (A and B) Data represent mean ± SE of 10 mice per group.

Figure 6. Anti-PD-L1 and anti-PD-1 treatments target $PD\text{-}1^+$ $CD8^+$ T cells that are induced by anti-CD4 treatment.

Mice bearing B16F10 tumors were treated with anti-CD4, anti-PD-L1 or anti-PD-1 mAbs, or a combination of these according to the treatment schedule shown in Fig. 4A. (A) Flow cytometry plots of blood $CD8^+$ T cells. (B and E) Proportions of $CD44^{hi}$ $PD\text{-}1^+$ cells, $PD\text{-}1^+$ $CD137^+$ cells or $CD44^{hi}$ $CD137^+$ cells among blood $CD8^+$ T cells on day 14. (C and F) Mean fluorescent intensity (MFI) of PD-1 expression on $CD8^+$ $CD44^{hi}$ $PD\text{-}1^+$ cells in the blood. (D and G) Proportions of $PD\text{-}1^+$ cells among tumor-infiltrating $CD8^+$ T cells. (B–D) show anti-PD-L1 mAb experiments; (E–G) show anti-PD-1 mAb experiments. Data represent mean ± SE of 4 mice per group and are representative of two independent experiments. *, $P < 0.05$; **, $P < 0.01$; ***, $P < 0.001$.

Author Manuscript Published OnlineFirst on February 20, 2015; DOI: 10.1158/2326-6066.CIR-14-0190
Author manuscripts have been peer reviewed and accepted for publication but have not yet been edited.

Fig. 1

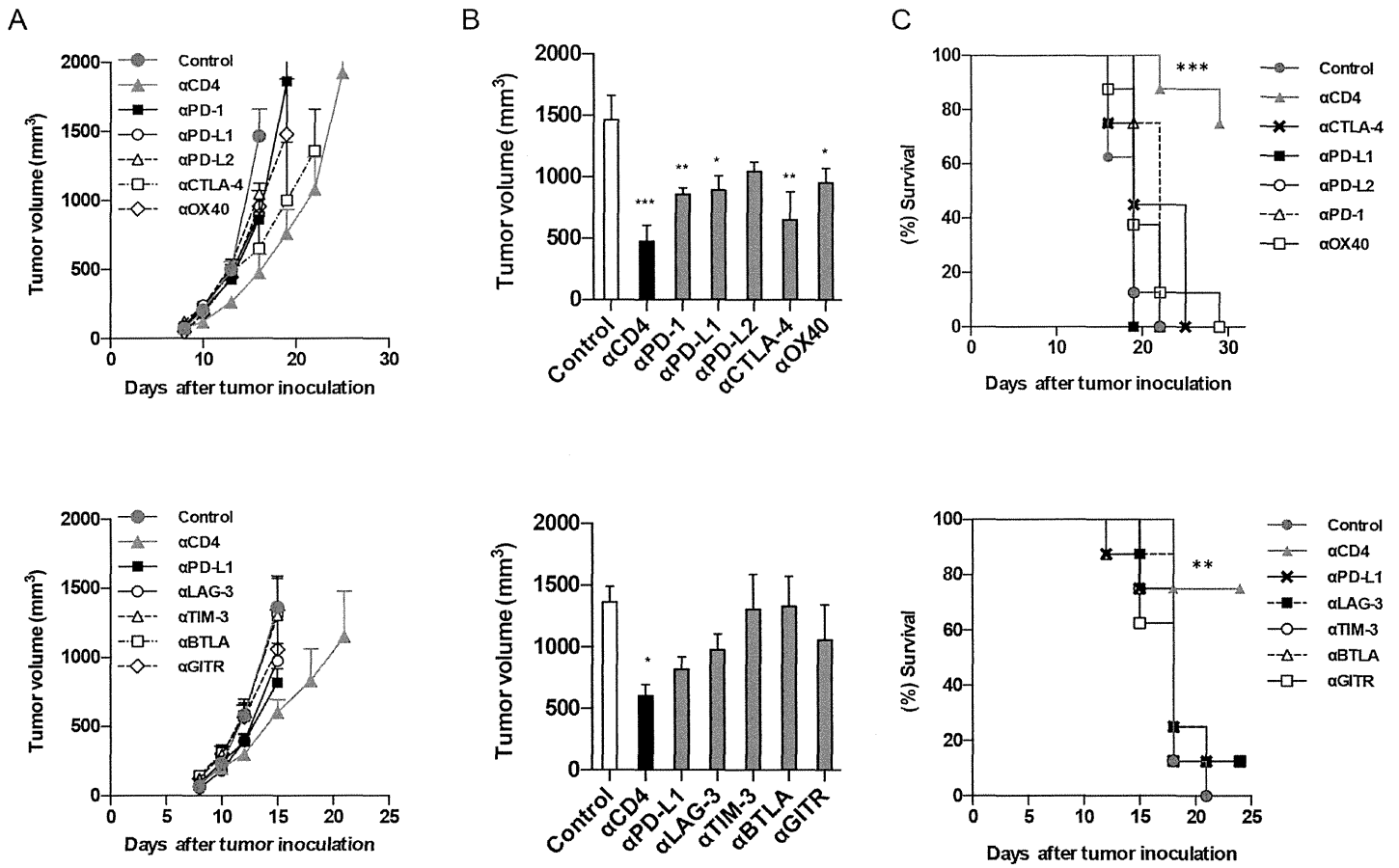

Author Manuscript Published OnlineFirst on February 20, 2015; DOI: 10.1158/2326-6066.CIR-14-0190
Author manuscripts have been peer reviewed and accepted for publication but have not yet been edited.

Fig. 2

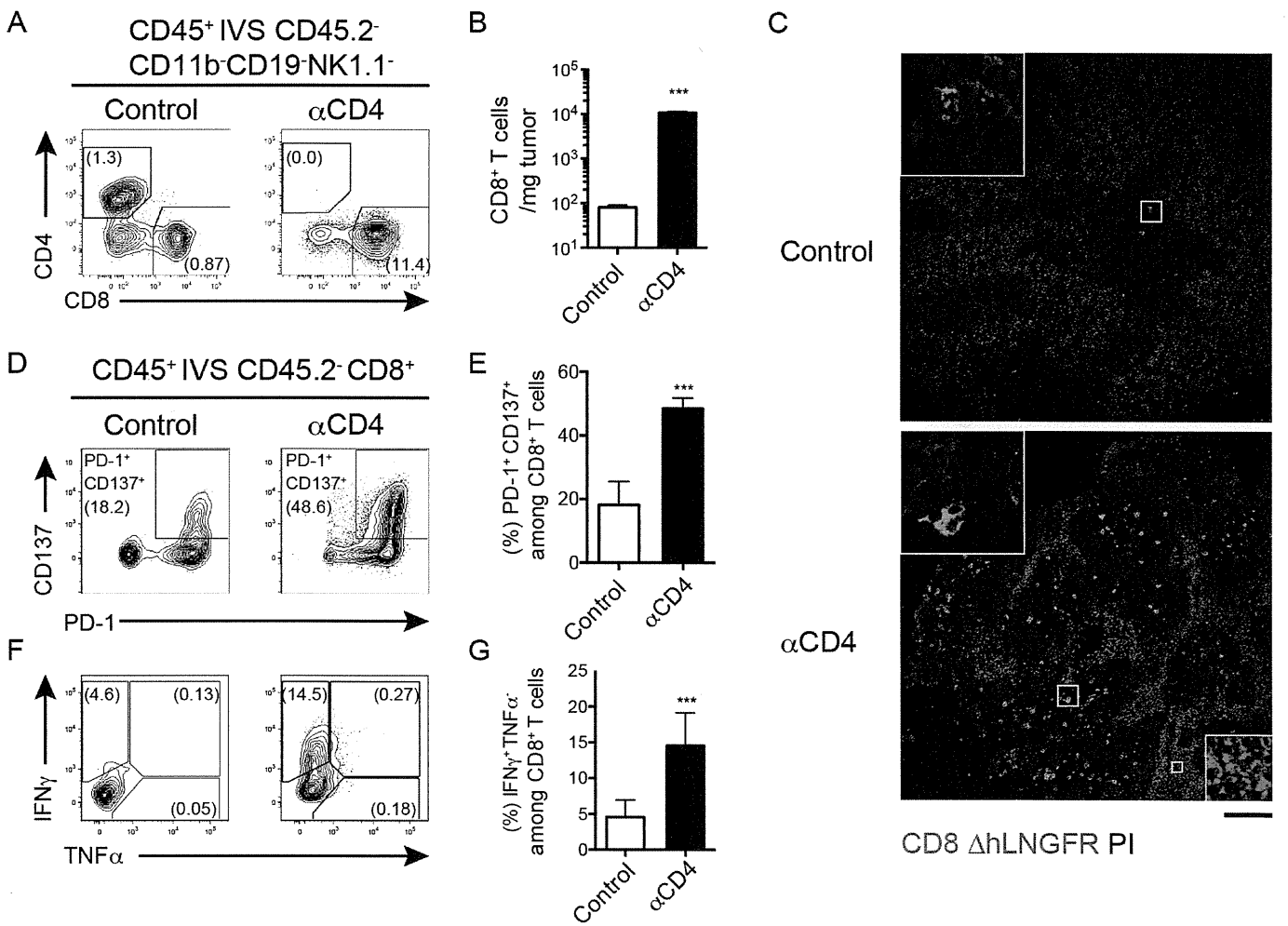

Author Manuscript Published OnlineFirst on February 20, 2015; DOI: 10.1158/2326-6066.CIR-14-0190
Author manuscripts have been peer reviewed and accepted for publication but have not yet been edited.

Fig. 3